

Capacity-achieving sparse superposition codes with spatially coupled VAMP decoder

Yuhao Liu, Teng Fu, Jie Fan, Panpan Niu, Chaowen Deng and Zhongyi Huang[†]

Department of Mathematical Sciences, Tsinghua University, Beijing, China

Email: {yh-liu21, fut21, fanj21, npp21 and dcw21}@mails.tsinghua.edu.cn, zhongyih@tsinghua.edu.cn

Abstract—Sparse superposition (SS) codes provide an efficient communication scheme over the Gaussian channel, utilizing the vector approximate message passing (VAMP) decoder for rotational invariant design matrices [1]. Previous work has established that the VAMP decoder for SS achieves Shannon capacity when the design matrix satisfies a specific spectral criterion and exponential decay power allocation is used [2]. In this work, we propose a spatially coupled VAMP (SC-VAMP) decoder for SS with spatially coupled design matrices. Based on state evolution (SE) analysis, we demonstrate that the SC-VAMP decoder is capacity-achieving when the design matrices satisfy the spectra criterion. Empirically, we show that the SC-VAMP decoder outperforms the VAMP decoder with exponential decay power allocation, achieving a lower section error rate. All codes are available on <https://github.com/yztfu/SC-VAMP-for-Superposition-Code.git>.

I. INTRODUCTION

Sparse superposition (SS) codes, also called sparse regression codes, were originally proposed by Barron and Joseph for reliable communication over the additive white Gaussian noise channel (AWGNC) [3]–[5]. While the scheme was known to be capacity-achieving for error correction with (intractable) maximum likelihood decoder [6], its computational complexity grows exponentially with code lengths. To mitigate this, the adaptive successive hard-decision decoder, a polynomial-time decoder, was proposed in [7], [8]. However, both theoretical and empirical performances remain suboptimal: the asymptotic results do not extend to practical finite section lengths, and the empirical section error rate at feasible code lengths remains high for rates near capacity.

An iterative soft-decision decoder for SS based on approximate message passing (AMP) algorithm [9], [10], with polynomial computational complexity, was proposed in [11], showing improved error performance at finite code lengths. The AMP decoder for SS, with power allocation (PA) or spatially coupled (SC) Gaussian design matrix, was shown asymptotically capacity-achieving through non-rigorous replica symmetric potential analysis [12], [13]. This was later fully rigorously proven by Rush et al., using conditional techniques, establishing that the AMP decoder achieves Shannon capacity over AWGNC and provides non-asymptotic section error rate bounds [14]–[16]. Similar analysis can be extended to show that the AMP decoder for SS with SC Gaussian design matrix,

based on generalized AMP (GAMP) algorithm [17], [18], is capacity-achieving over memoryless channels [19], [20].

In practice, non-Gaussian design matrix, such as Hadamard and discrete cosine transform (DCT) matrices [21], which are well approximated by orthogonally invariant matrices, can reduce the computational complexity for AMP decoder. However, the analysis in [14] does not hold for orthogonally invariant matrices. To address this, [1] proposed a decoder for SS with more structured design matrices, namely, right orthogonally invariant matrices, based on vector approximate message passing (VAMP) algorithm [22] (also known as orthogonal approximate message passing, OAMP [23]). They conjectured that VAMP decoder for SS is capacity-achieving if the design matrices satisfy the spectra criterion [1]. Subsequently, [2] rigorously proved that VAMP decoder for SS equipped with exponential decay PA is capacity-achieving under this spectra criterion and provided a non-asymptotic performance characterization of section error rate.

However, the empirical performance of SS with exponential decay PA remains unsatisfactory. Inspired by the superior practical performance of SS with spatially coupled (SC) Gaussian design matrices [12], [24], we introduce, for the first time, a spatially coupled VAMP (SC-VAMP) decoder for SS with spatially coupled rotational invariant design matrices. We first derive the SC-VAMP decoder using the factor graph [25] and the expectation consistent (EC) algorithm [26], [27]. Next, we demonstrate that the SC-VAMP decoder with design matrices satisfying the spectral criterion is capacity-achieving over AWGNC by state evolution (SE) analysis in the large-section limit. Finally, we empirically show that the SC-VAMP decoder outperforms the VAMP decoder with exponential decay PA for SS [2], achieving a lower section error rate.

Notation: We denote by $[n]$ the set $\{1, 2, \dots, n\}$ for a positive integer n . For a matrix $\mathbf{A} \in \mathbb{R}^{m \times m}$, we define $\langle \mathbf{A} \rangle$ as $m^{-1} \text{Tr}(\mathbf{A})$, where $\text{Tr}(\mathbf{A})$ represents the trace of \mathbf{A} . For a set S , $|S|$ denotes its cardinality. If a vector \vec{p} is partitioned into C blocks, $\vec{p} = [p_1, \dots, p_C]$, we use $\vec{p}[c]$ to refer to the c -th block p_c . Additionally, we define $\vec{x} = \text{concate}\{\mathbf{x}_c | c \in S\}$ as the vector \vec{x} obtained by concatenating \mathbf{x}_c for $c \in S$ in ascending order of the indices.

II. SPATIALLY COUPLED SS CONSTRUCTION

In the context of SS codes, the *message* vector $\mathbf{x} = [\mathbf{x}_{\text{sec}(1)}, \dots, \mathbf{x}_{\text{sec}(L)}] \in \mathbb{R}^N$ consists of L sections, each with

The first two authors contributed equally to this work and [†] marked the corresponding author.

B entries, where B is the *section size* and $N = LB$. The set $\text{sec}(l) := \{(l-1)B+1, \dots, lB\}$ collects the indices in the l -th section, with $\mathbf{x}_{\text{sec}(l)} = [x_{(l-1)B+1}, \dots, x_{lB}]$. Each section $\mathbf{x}_{\text{sec}(l)}, l \in \{1, \dots, L\}$ contains a single non-zero component, equal to one, whose position encodes the symbol to be transmitted. In the spatially coupled SS (SC-SS), the message is divided into C blocks equally, each containing L/C sections, such that $\mathbf{x} = [\mathbf{x}_1, \dots, \mathbf{x}_C]$. Each block $\mathbf{x}_c, c \in [C]$ concatenates the l_c -th section to r_c -th section, i.e., $\mathbf{x}_c = [\mathbf{x}_{\text{sec}(l_c)}, \dots, \mathbf{x}_{\text{sec}(r_c)}]$ where $l_c = (c-1)L/C + 1$ and $r_c = cL/C$. A *codeword* $\mathbf{z} = [\mathbf{z}_1, \dots, \mathbf{z}_R] \in \mathbb{R}^M$ is divided into R blocks equally, with each block \mathbf{z}_r generated from a fixed *design matrix* $\mathbf{A}_r \in \mathbb{R}^{M_r \times N_r}$, such that $\mathbf{z}_r = \mathbf{A}_r \tilde{\mathbf{x}}_r$, for $r \in [R]$. The vector $\tilde{\mathbf{x}}_r$ concatenates the blocks \mathbf{x}_c encoded by \mathbf{A}_r , with the indices of these blocks collected in W_r , such that $M_r = M/R$ and $N_r = N|W_r|/C$ and $\tilde{\mathbf{x}}_r = \text{concat}(\{\mathbf{x}_c | c \in W_r\})$. We consider random codes generated by \mathbf{A}_r , where \mathbf{A}_r is drawn from rotational invariant ensembles, i.e., the singular value decomposition $\mathbf{A}_r = \mathbf{U}_r \sqrt{\mathbf{S}_r} \mathbf{V}_r^T$ involves orthogonal bases \mathbf{U}_r and \mathbf{V}_r sampled uniformly from the orthogonal group $\mathcal{O}(M_r)$ and $\mathcal{O}(N_r)$, respectively. The diagonal matrix \mathbf{S}_r contains the squares of the singular values of \mathbf{A}_r , denoted $(S_{ri})_{i \leq N_r}$, on its main diagonal. The empirical distribution $N_r^{-1} \sum_{i \leq N_r} \delta_{S_{ri}}$ weakly converges to a well-defined, compactly supported probability density function as $N_r, M_r \rightarrow \infty$ (not necessarily proportionally). We denote the aspect ratio of \mathbf{A}_r as $\alpha_r = M_r/N_r$ ($0 < \alpha_r < 1$ generally) and $\rho_r = (1 - \alpha_r)\delta_0 + \alpha_r \rho_{\text{supp},r}$ the limit spectral density of $B^{-1} \mathbf{A}_r^T \mathbf{A}_r$, with $\rho_{\text{supp},r}$ the limit spectral density on \mathbb{R}^+ as $L \rightarrow \infty$. The overall (design) rate of the SC-SS is $R_{\text{all}} = L \log(B)/M = N \log(B)/(MB)$, and the rate associated with \mathbf{z}_r is $R_r = N_r \log(B)/(M_r B) = R|W_r|R_{\text{all}}/C$. Thus, the code is fully specified by the tuple $(M, R_{\text{all}}, B, R, C, \{W_r, \rho_r\}_{r=1}^R)$. In this paper, we set $C = \Gamma, R = \Gamma + W - 1$ and $\vartheta = (\Gamma + W - 1)/\Gamma$, considering the following $\{W_r\}_{r=1}^R$ inspired by the coupling structure shown in [12], [16], [19], [28], [29]

$$W_r = \begin{cases} \{1, 2, \dots, r\}, & 1 \leq r < W, \\ \{r - W + 1, \dots, r\}, & W \leq r \leq \Gamma, \\ \{r + 1 - W, \dots, \Gamma\}, & \Gamma < r \leq \Gamma + W - 1. \end{cases}$$

With this structure, a SC-SS can be defined by the tuple $(M, R_{\text{all}}, B, \Gamma, W, \{\rho_r\}_{r=1}^{\Gamma+W-1})$. For example, a SC-SS with parameters $\Gamma = 5, W = 2$ is shown in Fig. 1. For the sake of clarity and convenience, we will interchangeably use C and Γ , as well as R and $\Gamma + W - 1$, in the following context.

We enforce the power constraint $\|\mathbf{z}\|_2^2/M = 1 + o_L(1)$ by tuning \mathbf{A}_r 's spectrum to satisfy $\sum_{r=1}^R \int \lambda \rho_{\text{supp},r}(\lambda) d\lambda = R$ in the large L limit. In this paper, we adopt the simplified setting that $\int \lambda \rho_{\text{supp},r}(\lambda) d\lambda = 1$, ensuring $\|\mathbf{z}_r\|_2^2/M_r = 1 + o_L(1)$ for all $r \in [R]$. Codewords are transmitted through an AWGNC, i.e., the received corrupted codewords are $\mathbf{y} = \mathbf{z} + \mathbf{n}$ with i.i.d. $n_i \sim \mathcal{N}(0, \sigma^2), i \leq M$, so that the signal-to-noise ratio is $\text{snr} = \sigma^{-2}$. Then Shannon capacity of AWGNC is $\mathcal{C} = \log(1 + \text{snr})/2$. In communication systems, one usually prefers right

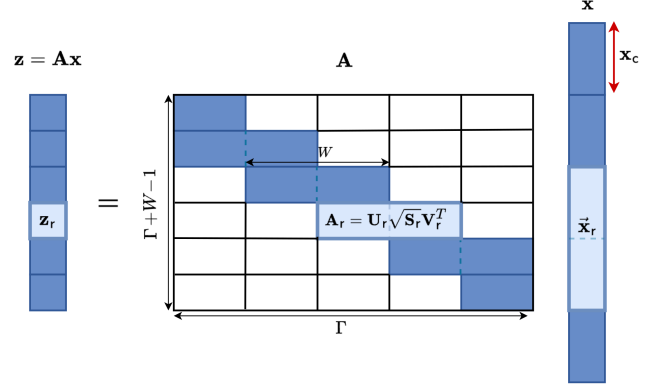


Fig. 1. A SC-SS with spatial coupling parameters $\Gamma = 5$ and $W = 2$, thus $R = 6, C = 5$ and $\vartheta = 6/5$. Each \mathbf{x}_c consists of L/Γ for $c \in [C]$, and each $\tilde{\mathbf{x}}_r$ consists of $|W_r|L/\Gamma$ sections for $r \in [R]$. Each design matrix \mathbf{A}_r contains $M/(\Gamma + W - 1)$ rows and $N|W_r|/\Gamma$ columns for $r \in [R]$.

rotational invariant ensembles $\mathbf{A}_r = \sqrt{\mathbf{S}_r} \mathbf{V}_r^T$. The choice does not affect the theoretical analysis, since we can left-multiply \mathbf{y}_r by $\text{diag}(\{\mathbf{U}_r\}_{r=1}^R)$ without altering the distributions of \mathbf{z} and noise \mathbf{n} .

III. SC-VAMP-BASED DECODER FOR SC-SS CODES

The minimum mean-square error (MMSE) estimator, which demonstrates excellent performance [6], is given by the expectation of the Bayes posterior

$$P(\mathbf{x}|\mathbf{y}, \{\mathbf{A}_r\}_{r=1}^R) \propto \prod_{r \leq R} e^{-\frac{\text{snr}}{2} \|\mathbf{y}_r - \mathbf{A}_r \tilde{\mathbf{x}}_r\|_2^2} \prod_{l \leq L} P_0(\mathbf{x}_{\text{sec}(l)}).$$

The hard constraints for the sections of the message are enforced by the prior distribution $P_0(\mathbf{x}_{\text{sec}(l)}) = B^{-1} \sum_{i \in \text{sec}(l)} \delta_{x_i, 1} \prod_{j \in \text{sec}(l), j \neq i} \delta_{x_j, 0}$. However, direct calculation of the Bayes posterior expectation is intractable due to the high dimensional integration with time complexity $O(B^L)$. The proposed SC-VAMP algorithm (see Algorithm 1) computes the MMSE estimator with polynomial time complexity.

VAMP was originally derived for generalized linear estimation [22], [23], and subsequently extended with a spatial coupling structure to achieve the information-theoretic compressing limitation [28]. We utilize the factor graph shown in Fig. 2, based on the EC algorithm to derive the SC-VAMP decoder for SS code. The primary distinction from the factor graph in [22] is that the variable factor \mathbf{x}_c is connected to multiple function factors δ_r . To address this modification, we employ uniform diagonalization [30], i.e., replacing the original message $\mathcal{N}(\tilde{\mathbf{x}}; \tilde{\mathbf{x}}_{2,r}^k, \text{diag}(\{(\hat{\eta}_{2,c}^k)^{-1} \mathbf{I} | c \in W_r\}))$ passed from the variable factors \mathbf{x}_c to the function factor δ_r with the approximation $\mathcal{N}(\tilde{\mathbf{x}}; \tilde{\mathbf{x}}_{2,r}^k, (\eta_{2,r}^k)^{-1} \mathbf{I}_{N_r})$, where $\eta_{2,r}^k = |W_r| / [\sum_{c \in W_r} (\hat{\eta}_{2,c}^k)^{-1}]$. This modification leads to the concatenating part in Algorithm 1.

With message passing rules [22] and uniform diagonalization, we derive the SC-VAMP for SS codes where the only difference from canonical SC-VAMP is that the so-called nonlinear denoiser $\mathbf{g}_2(\mathbf{p}, \gamma)$ acts section-wise rather than component wise. In full generality, the denoiser is defined as $\mathbf{g}_2(\mathbf{p}, \gamma) =$

Algorithm 1 SC-VAMP-based decoder for SC-SS codes

Require: Max iteration K , design matrices $\{\mathbf{A}_r\}_r^R$, noised codeword \mathbf{y}

```

1: Initialize  $\tilde{\mathbf{p}}_{1,r}^0 = \mathbf{0}$ ,  $\gamma_{1,r}^0 = B$  for  $r \in [R]$ 
2: for  $k = 0, 1, \dots, K$  do
3:   // LMMSE estimation
4:   for  $r = 1, \dots, R$  do
5:      $\tilde{\mathbf{x}}_{1,r}^k = \mathbf{g}_1(\tilde{\mathbf{p}}_{1,r}^k, \gamma_{1,r}^k, \mathbf{y}_r, \mathbf{A}_r)$ 
6:      $\alpha_{1,r}^k = \langle \mathbf{g}'_1(\tilde{\mathbf{p}}_{1,r}^k, \gamma_{1,r}^k, \mathbf{y}_r, \mathbf{A}_r) \rangle$ 
7:      $\eta_{1,r}^k = \gamma_{1,r}^k / \alpha_{1,r}^k$ 
8:      $\gamma_{2,r}^k = \eta_{1,r}^k - \gamma_{1,r}^k$ 
9:      $\tilde{\mathbf{p}}_{2,r}^k = (\eta_{1,r}^k \tilde{\mathbf{x}}_{1,r}^k - \gamma_{1,r}^k \tilde{\mathbf{p}}_{1,r}^k) / \gamma_{2,r}^k$ 
10:  // Denoising
11:  for  $\mathbf{c} = 1, \dots, \mathbf{C}$  do
12:     $\hat{\gamma}_{2,\mathbf{c}}^k = \sum_{r=\mathbf{c}}^{\mathbf{c}+W-1} \gamma_{2,r}^k$ 
13:     $\hat{\mathbf{p}}_{2,\mathbf{c}}^k = (\sum_{r=\mathbf{c}}^{\mathbf{c}+W-1} \gamma_{2,r}^k \tilde{\mathbf{p}}_{2,r}^k [\mathbf{c} + N(r) - r]) / \hat{\gamma}_{2,\mathbf{c}}^k$ 
14:     $(N(r) = |W_r| \mathbb{I}\{r \leq W\} + W \mathbb{I}\{r > W\})$ 
15:     $\hat{\mathbf{x}}_{2,\mathbf{c}}^k = \mathbf{g}_2(\hat{\mathbf{p}}_{2,\mathbf{c}}^k, \hat{\gamma}_{2,\mathbf{c}}^k)$ 
16:     $\hat{\alpha}_{2,\mathbf{c}}^k = \langle \mathbf{g}'_2(\hat{\mathbf{p}}_{2,\mathbf{c}}^k, \hat{\gamma}_{2,\mathbf{c}}^k) \rangle$ 
17:     $\hat{\eta}_{2,\mathbf{c}}^k = \hat{\gamma}_{2,\mathbf{c}}^k / \hat{\alpha}_{2,\mathbf{c}}^k$ 
18:  // Concatenating
19:  for  $r = 1, \dots, R$  do
20:     $\tilde{\mathbf{x}}_{2,r}^k = \text{concat}(\{\hat{\mathbf{x}}_{2,\mathbf{c}}^k | \mathbf{c} \in W_r\})$ 
21:     $\eta_{2,r}^k = |W_r| / [\sum_{\mathbf{c} \in W_r} (\hat{\eta}_{2,\mathbf{c}}^k)^{-1}]$ 
22:     $\gamma_{1,r}^{k+1} = \eta_{2,r}^k - \gamma_{2,r}^k$ 
23:     $\tilde{\mathbf{p}}_{1,r}^{k+1} = (\eta_{2,r}^k \tilde{\mathbf{x}}_{2,r}^k - \gamma_{2,r}^k \tilde{\mathbf{p}}_{2,r}^k) / \gamma_{1,r}^{k+1}$ 
24: return  $\{\tilde{\mathbf{x}}_{\mathbf{c}}^K\}_{\mathbf{c}=1}^{\mathbf{C}}$  (we define  $\tilde{\mathbf{x}}_{\mathbf{c}}^k = \hat{\mathbf{x}}_{2,\mathbf{c}}^k$  for  $\mathbf{c} \in [\mathbf{C}]$ )

```

$\mathbb{E}[\mathbf{X}|\mathbf{P} = \mathbf{p}]$ for the random variable $\mathbf{P} = \mathbf{X} + \sqrt{\gamma}^{-1} \mathbf{Z}$ with $\mathbf{X} \sim P_0^{\otimes(L/C)}$ and $\mathbf{Z} \sim \mathcal{N}(0, \mathbf{I}_{N/C})$. Plugging P_0 yields a component-wise expression for the denoiser and its variance:

$$\begin{cases} [g_2(\mathbf{p}, \gamma)]_i = \frac{\exp(\gamma p_i)}{\sum_{j \in \text{sec}(l_i)} \exp(\gamma p_j)}, \\ [g'_2(\mathbf{p}, \gamma)]_i = \gamma [g_2(\mathbf{p}, \gamma)]_i (1 - [g_2(\mathbf{p}, \gamma)]_i), \end{cases}$$

where $[g'_2(\mathbf{p}, \gamma)]_i := \partial_{p_i} [g_2(\mathbf{p}, \gamma)]_i$, l_i is the index of the section to which the i -th scalar component belongs. $\mathbf{g}_2(\tilde{\mathbf{p}}, \gamma, \mathbf{y}, \mathbf{A})$ can be interpreted as the MMSE estimate of the random vector $\tilde{\mathbf{x}}$ given the observation $\mathbf{y} \in \mathbb{R}^m$ and the matrix $\mathbf{A} \in \mathbb{R}^{m \times n}$, with $\mathbf{y} \sim \mathcal{N}(\mathbf{A}\tilde{\mathbf{x}}, \text{snr}^{-1} \mathbf{I}_n)$ and the prior is $\tilde{\mathbf{x}} \sim \mathcal{N}(\tilde{\mathbf{p}}, \gamma^{-1} \mathbf{I}_n)$:

$$\begin{cases} \mathbf{g}_1(\tilde{\mathbf{p}}, \gamma, \mathbf{y}, \mathbf{A}) = (\text{snr} \mathbf{A}^T \mathbf{A} + \gamma \mathbf{I}_n)^{-1} (\text{snr} \mathbf{A}^T \mathbf{y} + \gamma \tilde{\mathbf{p}}), \\ \langle \mathbf{g}'_1(\tilde{\mathbf{p}}, \gamma, \mathbf{y}, \mathbf{A}) \rangle = \gamma n^{-1} \text{Tr} \left[(\text{snr} \mathbf{A}^T \mathbf{A} + \gamma \mathbf{I}_n)^{-1} \right]. \end{cases}$$

The primary computational cost in the SC-VAMP decoder stems from the matrix inversion in the estimator \mathbf{g}_2 , which results in a time complexity of $O(B^3 L^3)$ per iteration. However, if all singular values of \mathbf{A} are equal to \sqrt{a} , \mathbf{g}_1 can be simplified as follows:

$$\mathbf{g}_1(\tilde{\mathbf{p}}, \gamma, \mathbf{y}, \mathbf{A}) = \tilde{\mathbf{p}} + \frac{\text{snr}}{\gamma + a \text{snr}} \mathbf{A}^T (\mathbf{y} - \mathbf{A} \tilde{\mathbf{p}}).$$

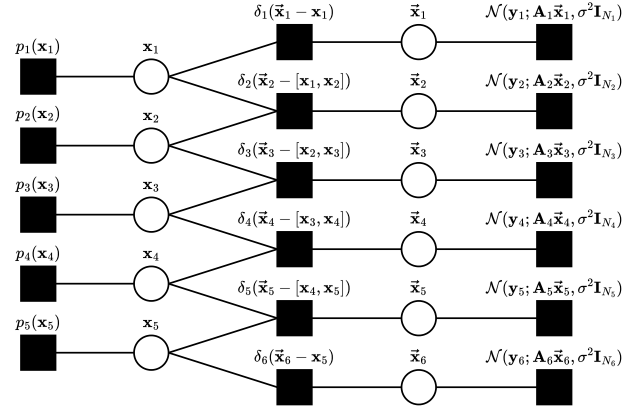


Fig. 2. Factor graph representation of the joint probability distribution of $\{\mathbf{x}_c\}_{\mathbf{c}}^{\mathbf{C}}$ and $\{\tilde{\mathbf{x}}_r\}_r^R$, with spatial coupling parameters $\Gamma = 5, W = 2$ and $\vartheta = 6/5$. The function factors $\{p_c(\cdot)\}_{\mathbf{c}}^{\mathbf{C}}$ represent $P_0^{\otimes(L/C)}$, and the factors $\{\delta_r(\cdot)\}_r^R$ represent the Dirac delta distributions.

In this case, the main computational cost is reduced to matrix-vector multiplication. Furthermore, if the design matrices $\{\mathbf{A}\}_{r=1}^R$ are generated from structured matrices, such as DCT matrices or Hadamard matrices [31], the overall time complexity per iteration is reduced to $O((BL) \log(BL))$.

IV. STATE EVOLUTION ANALYSIS

To evaluate the performance of the SC-VAMP estimator $\tilde{\mathbf{x}}_{\mathbf{c}} = (\tilde{x}_{l_{\mathbf{c}}}, \dots, \tilde{x}_{r_{\mathbf{c}}})$, we define two key error metrics for each block: the mean squared error (MSE) per section, denoted by $\{E_{\mathbf{c}}^k\}_{\mathbf{c}=1}^{\mathbf{C}}$ and the section error rate (SER), denoted by $\{\text{SER}_{\mathbf{c}}^k\}_{\mathbf{c}=1}^{\mathbf{C}}$. These metrics are expressed as follows:

$$E_{\mathbf{c}}^k = \frac{C}{L} \|\tilde{\mathbf{x}}_{\mathbf{c}}^k - \mathbf{x}_{\mathbf{c}}\|_2^2, \quad \text{SER}_{\mathbf{c}}^k = \frac{C}{L} \sum_{l=l_{\mathbf{c}}}^{r_{\mathbf{c}}} \mathbb{I}\{\tilde{x}_{\text{sec}(l)} \neq x_{\text{sec}(l)}\},$$

for $\mathbf{c} \in [\mathbf{C}]$, where $\mathbb{I}\{\cdot\}$ is the indicator function. In the asymptotic $L \rightarrow \infty$ limit (with $\alpha, B, R_{\text{all}}$ fixed), the MSE metric can be tracked by the following SE equations

$$\begin{aligned} \bar{\eta}_{1,r}^k &= [\mathcal{E}_{1,r}(\bar{\gamma}_{1,r}^k)]^{-1}, \quad \bar{\gamma}_{2,r}^k = \bar{\eta}_{1,r}^k - \bar{\gamma}_{1,r}^k, \quad r \in [R], \\ \bar{\gamma}_{2,\mathbf{c}}^k &= \sum_{r=\mathbf{c}}^{\mathbf{c}+W-1} \bar{\gamma}_{2,r}^k, \quad \bar{\eta}_{2,\mathbf{c}}^k = [\mathcal{E}_2(\bar{\gamma}_{2,\mathbf{c}}^k)/B]^{-1}, \quad \mathbf{c} \in [\mathbf{C}], \\ \bar{\eta}_{2,r}^k &= |W_r| / \sum_{\mathbf{c} \in W_r} (\bar{\eta}_{2,\mathbf{c}}^k)^{-1}, \quad \bar{\gamma}_{1,r}^{k+1} = \bar{\eta}_{2,r}^k - \bar{\gamma}_{2,r}^k, \quad r \in [R], \end{aligned}$$

with initialization $\bar{\gamma}_{1,r}^0 = B$ for $r \in [R]$. Here, $\mathcal{E}_{1,r}(\gamma) = \mathbb{E}_{p_r}(\text{snr} B \lambda + \gamma)^{-1}$ and

$$\mathcal{E}_2(\gamma) = 1 - \mathbb{E} \left[\frac{e^{\sqrt{\gamma} U_1}}{e^{\sqrt{\gamma} U_1} + e^{-\gamma} \sum_{j=2}^B e^{\sqrt{\gamma} U_j}} \right]$$

with $U_1, \dots, U_B \stackrel{\text{i.i.d.}}{\sim} \mathcal{N}(0, 1)$. The error function $\mathcal{E}_2(\gamma)$ can be interpreted as the Bayes posterior variance, i.e., $\mathcal{E}_2(\gamma) = \mathbb{E} \|\mathbf{S} - \mathbb{E}[\mathbf{S}|\mathbf{S} + \sqrt{\gamma}^{-1} \mathbf{Z}]\|_2^2$ with $\mathbf{S} \sim P_0$ and $\mathbf{Z} \sim \mathcal{N}(0, \mathbf{I}_B)$. With initialization $\tilde{\mathbf{p}}_{1,r}^0 = \mathbf{0}, \gamma_{1,r}^0 = \bar{\gamma}_{1,r}^0 = B$ for $r \in [R]$, it follows that for any finite B , $\lim_{L \rightarrow \infty} E_{\mathbf{c}}^K = B(\bar{\eta}_{2,\mathbf{c}}^K)^{-1}$ almost surely for $\mathbf{c} \in [\mathbf{C}]$. Next, we analyze SE in the limit

of large section size, i.e., as $B \rightarrow \infty$ while keeping R_{all} fixed (necessarily $\alpha = \Theta(\log B/B) \rightarrow 0$). With initialization $\gamma_{1,r}^0 = \Theta(B)$, the order of $\bar{\eta}_{1,r}^k, \bar{\eta}_{2,c}^k, \bar{\eta}_{2,r}^k, \bar{\gamma}_{1,r}^k$ is $\Theta(B)$, while the order of $\bar{\gamma}_{2,r}^k$ and $\bar{\gamma}_{2,c}^k$ is $\Theta(\log B)$. Introducing the rescaled variables $\sigma_r^k = B/\bar{\gamma}_{1,r}^k$, $\tau_c^k = \log B/\bar{\gamma}_{2,c}^k$, $\psi_c^k = B/\bar{\eta}_{2,c}^k$, and $\phi_r^k = R_r \bar{\gamma}_{2,r}^k / \log B$, the limit SE equations are given by:

$$\phi_r^k = F_r(\sigma_r^k), \quad r \in [\mathbf{R}], \quad (1)$$

$$\tau_c^k = R_{\text{all}} \left[\sum_{r=c}^{c+W-1} \frac{\phi_r^k}{\vartheta |W_r|} \right]^{-1}, \quad c \in [\mathbf{C}], \quad (2)$$

$$\psi_c^k = \mathbb{I}\{\tau_c^k > \frac{1}{2}\}, \quad c \in [\mathbf{C}], \quad (3)$$

$$\sigma_r^{k+1} = \frac{1}{|W_r|} \sum_{c \in W_r} \psi_c^k, \quad r \in [\mathbf{R}], \quad (4)$$

with the initialization $\sigma_r^0 = 1$ for $r \in [\mathbf{R}]$. Here, we exploit the phase transition of $\mathcal{E}_2(\gamma)$ [13], [16], where $\lim_{B \rightarrow \infty} \mathcal{E}_2(\gamma) = \mathbb{I}\{(\lim_{B \rightarrow \infty} \log B/\gamma) > 1/2\}$ and $F_r(x) = \mathbb{E}_{\rho_{0,r}} \frac{\lambda}{\lambda x + \sigma^2}$ for $r \in [\mathbf{R}]$, where $\rho_{0,r}$ is the $\alpha_r \rightarrow 0$ limit of $\rho_{\text{supp},r}$. If all the limit to $\rho_{\text{supp},r}$ converges to the same ρ_0 (e.g., when \mathbf{A}_r is a Gaussian matrix or $\rho_{\text{supp},r}$ is independent of α_r and B [1], [32]), we define $F_r(x) = F(x) = \mathbb{E}_{\rho_0} \frac{\lambda}{\lambda x + \sigma^2}$. This allows us to track E_c^k with ψ_c^k in the large section limitation. In Proposition 1, we analyze the evolution of the limited SE.

Proposition 1. Consider the limit SE with the same $F_r(x) = F(x)$ and initialization $\sigma_r^0 = 1$ for $r \in [\mathbf{R}]$. We define $R_{\text{alg}} := F(1)/2$ and $R_{\text{IT}} := \int_0^1 F(x) dx/2$. Then we have

- If $R_{\text{all}} < \vartheta^{-1} R_{\text{alg}}$, then $\psi_c^1 = 0$ for $c \in [\mathbf{C}]$;
- If $\vartheta^{-1} R_{\text{alg}} < R_{\text{all}} < \vartheta^{-1} R_{\text{IT}}$ and

$$W > \max\{\lceil 1/l^*(\vartheta) \rceil, \lceil 1/h^*(\vartheta, \Delta) \rceil\}, \quad (5)$$

where $\Delta := \vartheta^{-1} R_{\text{IT}} - R_{\text{all}}$, $l^*(\vartheta)$ is the unique solution of the equation in $(0, 1)$:

$$l(x) = x - \ln x = \frac{\vartheta R_{\text{all}}}{R_{\text{alg}}} \quad (6)$$

and $h^*(\vartheta, \Delta)$ is the unique solution of the equation in $(0, 1)$:

$$h(x) = \int_0^x F(t) dt - F(1)x = 2\vartheta \Delta. \quad (7)$$

We have $\psi_c^k = \psi_{\Gamma-c+1}^k = 0$ for $1 \leq c \leq \min\{(k+1)g, \lceil \Gamma/2 \rceil\}$ where $g := \min\{\lceil h^*(\vartheta, \Delta)W \rceil, \lceil l^*(\vartheta)W \rceil\}$. Furthermore, after $K = 1 + \lceil \Gamma/(2g) \rceil$ iterations, we have $\psi_c^K = 0$ for $c \in [\mathbf{C}]$.

Proof. Since the variables ψ_c^k for $c \in [\Gamma]$ are symmetric about the center column index, i.e. $\psi_c = \psi_{\Gamma-c+1}$ for $c < \lceil \Gamma/2 \rceil$, we carry out the analysis for $c \in [\lceil \Gamma/2 \rceil]$ and $r \in [\lceil \Gamma/2 \rceil + W - 1]$. With initialization $\sigma_r^0 = 1$ for $r \in [\mathbf{R}]$, we have

$$\tau_c^0 = \frac{R_{\text{all}} \vartheta}{F(1)} \begin{cases} \left[\sum_{r=c}^{c+W-1} \frac{1}{r} + \frac{c}{W} \right]^{-1}, & 1 \leq c \leq W, \\ 1, & c > W. \end{cases}$$

Here, τ_c^0 is non-decreasing with the block index c . Thus, if $R_{\text{all}} < \vartheta^{-1} R_{\text{alg}}$, we have $\tau_c^0 \leq \frac{1}{2}$ implying $\psi_c^1 = 0$ for $c \in [\mathbf{C}]$.

Otherwise, if $\vartheta^{-1} R_{\text{alg}} < R_{\text{all}} < \vartheta^{-1} R_{\text{IT}}$. Firstly, we establish that $l(x)$ and $h(x)$ each have a unique solution on $(0, 1)$, respectively. Differentiating $l(x)$ over $(0, 1)$, we obtain $l'(x) = 1 - 1/x < 0$, implying $l(x)$ is decreasing for $0 < x < 1$. Given that $\lim_{x \rightarrow 0^+} l(x) = +\infty$ and $l(1) = 0 < (\vartheta R_{\text{all}})/R_{\text{alg}}$ with continuity of $l(x)$ in $(0, 1]$, it follows that equation (6) has a unique solution $l^*(\vartheta)$ on $(0, 1)$. We differentiate $h(x)$ over $[0, 1]$ to obtain

$$h'(x) = F(x) - F(1)$$

and since $F(x)$ is decreasing on $(0, 1)$, it follows that $h'(x) \geq 0$, implying $h(x)$ is increasing on $(0, 1)$. Moreover, with $h(0) = 0 < 2\vartheta \Delta$, $h(1) = 2(R_{\text{IT}} - R_{\text{alg}}) > 2\vartheta \Delta$ and the continuity of $h(x)$ on $[0, 1]$, we conclude that equation (7) has a unique solution $h^*(\vartheta, \Delta)$ in $(0, 1)$.

With the inequality $\sum_{r=c}^{W-1} (1/r) \leq \ln(W/c)$ for $1 \leq c \leq W$, we deduce the following inequality of τ_c^0 :

$$\tau_c^0 \leq \frac{R_{\text{all}} \vartheta}{F(1)} \begin{cases} \left[\frac{c}{W} - \ln(\frac{c}{W}) \right]^{-1}, & 1 \leq c \leq W, \\ 1, & c > W. \end{cases}$$

Since $l(x)$ is decreasing on $(0, 1)$, we have $\tau_c^0 < 1/2$, implying $\psi_c^0 = 0$ for $1 \leq c \leq g$ (g is a integer greater than or equal to 1 according to (5)).

Next we consider the subsequent iterations $k \geq 1$. Assume towards induction that $\psi_c^k = 0$ for $c \leq g^k$ where $g^k \geq (k+1)g$. Based on the assumption, we deduce the inequality for σ_r^{k+1} as follows:

$$\sigma_r^{k+1} \geq \begin{cases} 0, & r \leq g^k, \\ (r - g^k)/|W_r|, & g^k \leq r \leq g^k + W, \\ 1, & r > g^k + W. \end{cases}$$

Using the fact $F(x)$ is decreasing on $[0, 1]$ and (1), we obtain

$$\phi_r^{k+1} \geq \begin{cases} F(0), & r \leq g^k, \\ F((r - g^k)/|W_r|), & g^k \leq r \leq g^k + W, \\ F(1), & r > g^k + W. \end{cases}$$

Since ψ_c^k increases with the block index $c \in [\lceil \Gamma/2 \rceil]$, we have σ_r^{k+1} increases with the block index r for $r \in [\lceil \Gamma/2 \rceil + W - 1]$ according to (4). Given that $F(x)$ is decreasing on $[0, 1]$, we conclude that $\phi_r^{k+1}/|W_r| = F(\sigma_r^{k+1})/|W_r|$ decreases with the block index r for $r \in [\lceil \Gamma/2 \rceil + W - 1]$ according to (1). Therefore, τ_c^{k+1} increases with the block index c for $c \in [\lceil \Gamma/2 \rceil]$ according to (2). We now consider τ_c^{k+1} for $g^k < c \leq g^k + W$ as follows:

$$\frac{\tau_c^{k+1}}{R_{\text{all}} \vartheta} \leq \left[\sum_{r=c}^{g^k+W-1} \frac{F((r - g^k)/|W_r|)}{|W_r|} + \sum_{r=g^k+W}^{c+W-1} \frac{F(1)}{|W_r|} \right]^{-1}.$$

Since $xF(bx)$ is increasing on $[0, 1]$ for $b > 0$ and $|W_r| \leq W$ for $r \in [\mathbf{R}]$, we obtain the following inequality:

$$\frac{\tau_c^{k+1}}{R_{\text{all}} \vartheta} \leq \left[\sum_{r=c}^{g^k+W-1} \frac{F((r - g^k)/|W|)}{|W|} + \sum_{r=g^k+W}^{c+W-1} \frac{F(1)}{|W|} \right]^{-1}.$$

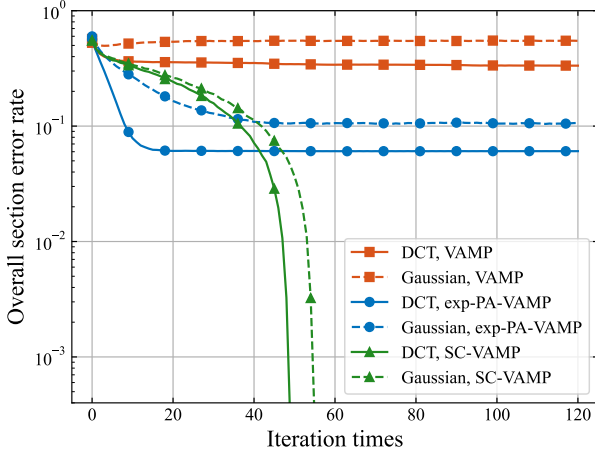


Fig. 3. Overall section error rate $\text{SER}^k = (\sum_{c=1}^C \text{SER}_c^k)/C$ ran on a random single instance with $L = 2^{14}$, $B = 16$ and $\text{snr} = 15$, as a function of the iterations. For SC-VAMP decoder, we set $\Gamma = 16$, $W = 2$ and $\vartheta = 17/16$. The overall rate $R_{\text{all}} = 1.60$ is higher than the algorithm threshold, lower than the information-theoretic threshold proposed in [1].

Given that $F(x)$ is decreasing in $[0, 1]$, we have

$$\tau_c^{k+1} \leq R_{\text{all}} \vartheta \left[\int_{\frac{c-g^k}{W}}^1 F(x) dx + \frac{c-g^k}{W} F(1) \right]^{-1}.$$

Finally, since $h(x)$ is decreasing on $(0, 1)$, it follows that $\tau_c^{k+1} \leq \frac{1}{2}$, implying $\psi_c^{k+1} = 0$ for $c \leq g^k + g$. Moreover, since $Kg \geq \lceil \Gamma/2 \rceil$, it follows that $\psi_c^K = 0$ for $c \in [C]$. \square

The Proposition 1 establishes that, under $R_{\text{all}} < \vartheta^{-1} R_{\text{IT}}$, the limit SE iteratively transitions ψ_c^k from 1 to 0, progressing from the outermost blocks toward the central blocks. And after K iterations, ψ_c^K reduces to 0 for all blocks. Moreover, for sufficiently large W with $\Gamma > W^2$, we have $\vartheta \rightarrow 1$ as $W \rightarrow \infty$. Consequently, Proposition 1 implies that perfect recovery of the message x is achievable when $R_{\text{all}} < R_{\text{IT}}$, thereby confirming the conjectures in [32].

Using Cauchy–Schwarz inequality, we obtain

$$\mathbb{E}_{\rho_0} \left(\frac{\lambda}{\lambda x + \sigma^2} \right) \mathbb{E}_{\rho_0} (\lambda x + \sigma^2) \leq \mathbb{E}_{\rho_0} \lambda,$$

where the equality holds if and only if $\rho_0 = \delta_1$. This implies that $F(x) \leq 1/(\sigma^2 + x)$, leading to the following bound:

$$R_{\text{IT}} \leq \frac{1}{2} \int_0^1 \frac{1}{\sigma^2 + x} dx = \frac{1}{2} \log(1 + \text{snr}) = \mathcal{C}.$$

Therefore, the SC-SS code with SC-VAMP decoder is capacity-achieving for AWGNC if all $\rho_{\text{supp},r}$ converges to δ_1 as $\alpha \rightarrow 0$, a condition referred to as the spectra criterion in [1], [2], [32].

V. NUMERICAL RESULTS

We present our numerical results using the following two design matrices:

- 1) **Gaussian matrices.** Each element of \mathbf{A}_r is i.i.d. drawn from $\mathcal{N}(0, L^{-1})$. The limit spectral distribution ρ_r fol-

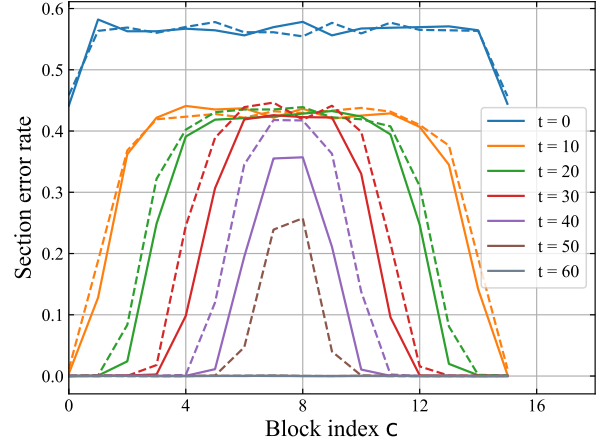


Fig. 4. SER_c^k vs. block index $c \in [C]$ for several iteration numbers in a SC-VAMP decoding process, using the same setup as in Fig.3. The solid line corresponds to DCT matrices, while the dotted line corresponds to Gaussian matrices.

lows the Marchenko–Pastur law, given by $\rho_r(\lambda) = (1 - \alpha_r) \delta_{\lambda,0} + \frac{\sqrt{(\lambda - \lambda_-)(\lambda_+ - \lambda)}}{2\pi\lambda}$, where $\lambda_r^\pm := (1 \pm \sqrt{\alpha_r})^2$.

- 2) **DCT matrices.** To simulate row-orthogonal matrices with the limiting spectral distribution $\rho_r(\lambda) = (1 - \alpha_r) \delta_{\lambda,0} + \alpha_r \delta_{\lambda,1}$, we randomly choose $M_r \leq N_r$ rows from a $N_r \times N_r$ DCT matrix.

In Fig. 3, we present a comparison between our SC-VAMP decoder, the original VAMP decoder [1], and the exp-PA-VAMP decoder, which incorporates exponential decay power allocation [2]. Our results show that the original VAMP decoder fails to decode successfully because R_{all} exceeds the algorithmic threshold. In contrast, both the SC-VAMP and the exp-PA-VAMP decoders achieve successful decoding. Notably, the SC-VAMP decoder demonstrates superior empirical performance, achieving an overall section error rate of less than 10^{-3} . Furthermore, we observe that DCT matrices consistently outperform Gaussian matrices.

Figure 4 illustrates the dynamics of the section error rate in the SC-VAMP decoding process. We observe that the SC-VAMP decoder successfully decodes progressively from the outermost blocks towards the central blocks, thereby confirming the validity of Proposition 1.

VI. FURTHER WORK

In practice, we aim to derive non-asymptotic section error rate bounds for $B, L \rightarrow \infty$ with appropriate scaling, e.g., $B = O(L^\alpha)$ and expect exponential decay of these bounds using techniques from [16], [33]–[35]. We also expect these results to extend to general memoryless channels, as suggested informally in [32] from a statistical physics perspective. Further open problems related to SC-SS include designing faster, more robust decoders based on message-passing algorithms in [36], [37], and analyzing the performance of SC-SS with more realistic design matrices, such as the class of semi-random matrices [38], [39].

REFERENCES

- [1] T. Hou, Y. Liu, T. Fu, and J. Barbier, "Sparse superposition codes under VAMP decoding with generic rotational invariant coding matrices," in *Proc. IEEE ISIT*, June 2022, pp. 1372–1377.
- [2] Y. Xu, Y. Liu, S. Liang, T. Wu, B. Bai, J. Barbier, and T. Hou, "Capacity-achieving sparse regression codes via vector approximate message passing," in *Proc. IEEE ISIT*, June 2023, pp. 785–790.
- [3] A. R. Barron and A. Joseph, "Toward fast reliable communication at rates near capacity with gaussian noise," in *Proc. IEEE ISIT*, June 2010, pp. 315–319.
- [4] A. R. Barron and A. Joseph, "Analysis of fast sparse superposition codes," in *Proc. IEEE ISIT*, July 2011, pp. 1772–1776.
- [5] A. Joseph and A. R. Barron, "Least squares superposition codes of moderate dictionary size are reliable at rates up to capacity," *IEEE Trans. Inf. Theory*, vol. 58, no. 5, pp. 2541–2557, May 2012.
- [6] R. Venkataramanan, S. Tatikonda, A. Barron *et al.*, "Sparse regression codes," *Found. Trends® Commun. Inf. Theory*, vol. 15, no. 1-2, pp. 1–195, 2019.
- [7] A. Joseph and A. R. Barron, "Fast sparse superposition codes have near exponential error probability for $R < C$," *IEEE Trans. Inf. Theory*, vol. 60, no. 2, pp. 919–942, Feb. 2014.
- [8] S. Cho and A. Barron, "Approximate iterative Bayes optimal estimates for high-rate sparse superposition codes," in *Sixth Workshop on Inf. The. Methods in Sci. and Eng.*, 2013, pp. 35–42.
- [9] D. L. Donoho, A. Maleki, and A. Montanari, "Message-passing algorithms for compressed sensing," *Proc. Natl. Acad. Sci. U.S.A.*, vol. 106, no. 45, pp. 18 914–18 919, 2009.
- [10] M. Bayati and A. Montanari, "The dynamics of message passing on dense graphs, with applications to compressed sensing," *IEEE Trans. Inf. Theory*, vol. 57, no. 2, pp. 764–785, Feb. 2011.
- [11] J. Barbier and F. Krzakala, "Replica analysis and approximate message passing decoder for superposition codes," in *Proc. IEEE ISIT*, June 2014, pp. 1494–1498.
- [12] J. Barbier and F. Krzakala, "Approximate message-passing decoder and capacity achieving sparse superposition codes," *IEEE Trans. Inf. Theory*, vol. 63, no. 8, pp. 4894–4927, Aug. 2017.
- [13] J. Barbier, M. Dia, and N. Macris, "Proof of threshold saturation for spatially coupled sparse superposition codes," in *Proc. IEEE ISIT*, July 2016, pp. 1173–1177.
- [14] C. Rush, A. Greig, and R. Venkataramanan, "Capacity-achieving sparse superposition codes via approximate message passing decoding," *IEEE Trans. Inf. Theory*, vol. 63, no. 3, pp. 1476–1500, Mar. 2017.
- [15] C. Rush and R. Venkataramanan, "The error probability of sparse superposition codes with approximate message passing decoding," *IEEE Trans. Inf. Theory*, vol. 65, no. 5, pp. 3278–3303, May 2019.
- [16] C. Rush, K. Hsieh, and R. Venkataramanan, "Capacity-achieving spatially coupled sparse superposition codes with AMP decoding," *IEEE Trans. Inf. Theory*, vol. 67, no. 7, pp. 4446–4484, July 2021.
- [17] S. Rangan, "Generalized approximate message passing for estimation with random linear mixing," in *Proc. IEEE ISIT*, July 2011, pp. 2168–2172.
- [18] O. Y. Feng, R. Venkataramanan, C. Rush, R. J. Samworth *et al.*, "A unifying tutorial on approximate message passing," *Found. Trends Mach. Learn.*, vol. 15, no. 4, pp. 335–536, 2022.
- [19] J. Barbier, M. Dia, and N. Macris, "Universal sparse superposition codes with spatial coupling and GAMP decoding," *IEEE Trans. Inf. Theory*, vol. 65, no. 9, pp. 5618–5642, Sep. 2019.
- [20] Y. Liu, Y. Xu, and T. Hou, "The error probability of spatially coupled sparse regression codes over memoryless channels," *arXiv preprint arXiv:2409.05745*, 2024.
- [21] A. Greig and R. Venkataramanan, "Techniques for improving the finite length performance of sparse superposition codes," *IEEE Trans. Commun.*, vol. 66, no. 3, pp. 905–917, Mar. 2017.
- [22] S. Rangan, P. Schniter, and A. K. Fletcher, "Vector approximate message passing," *IEEE Trans. Inf. Theory*, vol. 65, no. 10, pp. 6664–6684, Oct. 2019.
- [23] J. Ma and L. Ping, "Orthogonal AMP," *IEEE Access*, vol. 5, pp. 2020–2033, Jan. 2017.
- [24] K. Hsieh, C. Rush, and R. Venkataramanan, "Spatially coupled sparse regression codes: Design and state evolution analysis," in *Proc. IEEE ISIT*, June 2018, pp. 1016–1020.
- [25] F. R. Kschischang, B. J. Frey, and H.-A. Loeliger, "Factor graphs and the sum-product algorithm," *IEEE Trans. Inf. Theory*, vol. 47, no. 2, pp. 498–519, Feb. 2001.
- [26] T. P. Minka, "A family of algorithms for approximate Bayesian inference," Ph.D. dissertation, Dept. Elect. Eng. Comput. Sci., MIT, Cambridge, MA, USA, 2001.
- [27] M. Seeger, "Expectation propagation for exponential families," 2005. [Online]. Available: <https://infoscience.epfl.ch/handle/20.500.14299/61899>
- [28] K. Takeuchi, "Orthogonal approximate message-passing for spatially coupled linear models," *IEEE Trans. Inf. Theory*, vol. 70, no. 1, pp. 594–631, Jan. 2023.
- [29] P. P. Cobo, K. Hsieh, and R. Venkataramanan, "Bayes-optimal estimation in generalized linear models via spatial coupling," *IEEE Trans. Inf. Theory*, vol. 70, no. 11, pp. 8343–8363, Nov. 2024.
- [30] A. Fletcher, M. Sahraee-Ardakan, S. Rangan, and P. Schniter, "Expectation consistent approximate inference: Generalizations and convergence," in *Proc. IEEE ISIT*, July 2016, pp. 190–194.
- [31] A. Abbara, A. Baker, F. Krzakala, and L. Zdeborová, "On the universality of noiseless linear estimation with respect to the measurement matrix," *Journal of Physics A: Mathematical and Theoretical*, vol. 53, no. 16, p. 164001, 2020.
- [32] Y. Liu, T. Fu, J. Barbier, and T. Hou, "Sparse superposition codes with rotational invariant coding matrices for memoryless channels," in *Proc. IEEE ITW*, Nov. 2022, pp. 267–272.
- [33] C. Rush and R. Venkataramanan, "Finite sample analysis of approximate message passing algorithms," *IEEE Trans. Inf. Theory*, vol. 64, no. 11, pp. 7264–7286, Nov. 2018.
- [34] G. Li and Y. Wei, "A non-asymptotic framework for approximate message passing in spiked models," *arXiv preprint arXiv:2208.03313*, 2022.
- [35] C. Cademartori and C. Rush, "A non-asymptotic analysis of generalized vector approximate message passing algorithms with rotationally invariant designs," *IEEE Trans. Inf. Theory*, vol. 70, no. 8, pp. 5811–5856, Aug. 2024.
- [36] L. Liu, S. Huang, and B. M. Kurkoski, "Memory AMP," *IEEE Trans. Inf. Theory*, vol. 68, no. 12, pp. 8015–8039, Dec. 2022.
- [37] Z. Fan, "Approximate message passing algorithms for rotationally invariant matrices," *The Annals of Statistics*, vol. 50, no. 1, pp. 197–224, 2022.
- [38] R. Dudeja, Y. M. Lu, and S. Sen, "Universality of approximate message passing with semirandom matrices," *The Annals of Probability*, vol. 51, no. 5, pp. 1616–1683, 2023.
- [39] R. Dudeja, S. Sen, and Y. M. Lu, "Spectral universality in regularized linear regression with nearly deterministic sensing matrices," *IEEE Trans. Inf. Theory*, vol. 70, no. 11, pp. 7923–7951, Nov. 2024.